

# Supplemental Materials for “Inhibiting Responses to Difficult Choices”

Dora Matzke

Department of Psychology, University of Amsterdam, The Netherlands

Samuel Curley

School of Psychology, University of Newcastle, Australia

Charlene Q. Gong

King’s College Hospital, London

Andrew Heathcote

School of Medicine, University of Tasmania, Australia

Correspondence concerning this article should be addressed to:

Dora Matzke, Department of Psychology, PO Box 15906, 1001 NK Amsterdam, The Netherlands, E-mail: [d.matzke@uva.nl](mailto:d.matzke@uva.nl).

### Bayesian Inference

Figure 1 illustrates the basic concepts of Bayesian parameter estimation.

### Parameter Recovery Studies

#### Prior Specification

We used the following prior setting for the parameter recovery studies.

$$\mu_+, \mu_- \sim \text{Uniform}(0, 2),$$

$$\sigma_+, \sigma_- \sim \text{Uniform}(0, 2),$$

$$\tau_+, \tau_- \sim \text{Uniform}(0, 2),$$

$$\mu_S \sim \text{Uniform}(0, 2),$$

$$\sigma_S \sim \text{Uniform}(0, 2),$$

$$\tau_S \sim \text{Uniform}(0, 2),$$

$$P_{TF}, P_{GF} \sim \text{Uniform}(0, 1).$$

### Parameter Recovery in the Presence of Go Errors and Go Failures: Full Posterior Distributions

Figure 2 shows the bias in the parameter estimates as a result of go errors. Figure 3 show the bias in parameter estimates as a result of the simultaneous presence of go failures and go errors.

### Fitting Real-World Stop-Signal Data

#### Prior Specification

We modeled the parameters of each participant  $j$ ,  $j = 1, \dots, K$ , in the Easy (E) and Difficult (D) conditions with truncated-normal population-level distributions. The participant-level  $P_{TF}$  and  $P_{GF}$  parameters were first projected from the probability scale to the real line with a probit transformation.

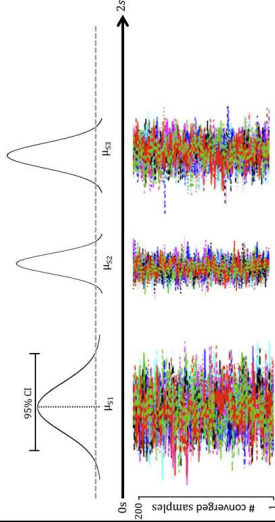
### Bayesian Parameter Estimation

Traditionally, model parameters are estimated for each individual separately, assuming that participants are completely independent. We start with a **prior distribution** for the model parameter of interest  $\Theta$ : the prior distribution  $p(\Theta)$  represents existing knowledge about this parameter. Using Bayes' rule, the prior distribution is then updated by the observed data  $\mathbf{D}$  (i.e., the likelihood) to arrive at the **posterior distribution**:  $p(\Theta|\mathbf{D}) = \frac{p(\mathbf{D}|\Theta)p(\Theta)}{p(\mathbf{D})}$ . The marginal likelihood in the denominator  $p(\mathbf{D}) = \int p(\mathbf{D}|\theta)p(\theta)d\theta$  is a normalizing constant that ensures that the posterior distribution integrates to one.

Figure 1A illustrates the basic concepts of Bayesian parameter estimation, using the  $\mu_{js}$  parameter of the standard BEESTS model (Mäzke, Dolan, Logan, Brown, & Wagenmakers, 2013) for three fictitious participants. The prior distribution (grey dashed line) is an uninformative uniform distribution that assigns equal prior probability mass to parameter values between 0 and 2. Note that Bayesian parameter estimation is robust to the choice of the prior, given sufficiently informative data (e.g., Lee & Wagenmakers, 2013). That is, as the informativeness of the data increases, the influence of the prior decreases, unless the prior allows no probability of particular values. The posterior distribution (black solid density lines) quantifies the uncertainty of the parameter estimate after the data have been observed. The central tendency of the posterior, such as its mean (dotted vertical line) can be used as a point estimate. The uncertainty of the estimate can be quantified with the 95% **credible interval** (CI) of the posterior (i.e., area between the 2.5<sup>th</sup> and 97.5<sup>th</sup> percentile of the distribution); the 95% CI encompasses the range of values that contains the true value of the parameter with 95% probability. Intuitively, the wider the 95% CI, the greater the uncertainty of the estimate.

For complex models, such as BEESTS, the posterior distribution cannot be derived analytically because the marginal likelihood features a multidimensional integral without closed form solution. The posterior distribution is, therefore, approximated using Markov chain Monte Carlo (MCMC) methods by drawing sequences of samples—**chains**—from the posterior. Figure 1B shows, for each participant, 18 MCMC chains each with 200 samples from the posterior distribution. The samples were obtained using the Differential Evolution sampler (Turner, Sederberg, Brown, & Steyvers, 2013). The posterior samples can be used to approximate the mean and CI of the posterior distribution.

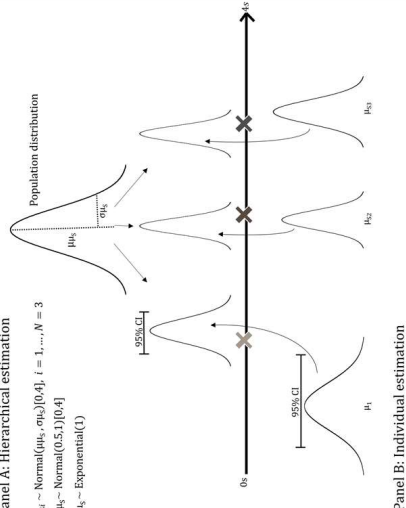
Panel A: Prior and posterior  
 $\mu_{js} \sim \text{Uniform}(0,2), j = 1, \dots, N = 3$



Panel B: MCMC sampling

Figure 1. MCMC-based Bayesian parameter estimation.

Panel A: Hierarchical estimation  
 $\mu_{j1} \sim \text{Normal}(\mu_{j1s}, \sigma_{j1s}^2)[0,4], j = 1, \dots, N = 3$   
 $\mu_{j2} \sim \text{Normal}(0.5, 1)[0,4]$   
 $\sigma_{j1s} \sim \text{Exponential}(1)$



Panel B: Individual estimation

Figure 2. Bayesian hierarchical modeling.

### Bayesian Hierarchical Modeling

Rather than estimating parameters for each participant separately, **Bayesian hierarchical modeling** assumes that participants share similarities and explicitly models individual differences in parameter values (e.g., Gelman & Hill, 2007; Matzke & Wagenmakers, 2009; Rouder, Lu, Speckman, Sun, & Jiang, 2005; Shiffrin, Lee, Kim, & Wagenmakers, 2008). Hierarchical modeling assumes that the individual model parameters are drawn from **population distributions** which describe how the **participant-level parameters** vary in the population. The population distributions are characterized by a set of **population-level parameters**, such as means and standard deviations, which provide inference on the group level. These population means and standard deviations generate the individual parameters as random effects and are assumed to be unknown. This implies that we set priors on the population parameters, which allows us to estimate them from the data.

Figure 2A illustrates the basic concepts of Bayesian hierarchical estimation for three fictitious participants. The hierarchical BEESTS model assumes that the  $\mu_{js}$  parameter of each participant  $j = 1, \dots, N = 3$ , is drawn from a truncated-normal population distribution restricted to values between 0 and 4:  $\mu_{js} \sim \text{Normal}(\mu_{j1s}, \sigma_{j1s}^2)[0,4]$ . The upper truncation is not necessarily, but can be computationally helpful. The population distribution is characterized by the population mean  $\mu_{j1s}$  and standard deviation  $\sigma_{j1s}$ . The prior for  $\mu_{j1s}$  is a truncated-normal distribution centered at 0.5, with standard deviation of 1:  $\mu_{j1s} \sim \text{Normal}(0.5, 1)[0,4]$ . This prior expresses certainty that  $\mu_{j1s}$  is between 0 and 4, but otherwise might take on a broad range of values. The prior for  $\sigma_{j1s}$  is an exponential distribution with rate of 1. This prior expresses certainty that the standard deviation is positive (as it must be) and assigns most prior mass to relatively low values.

Bayesian hierarchical estimation uses information from the population-level parameters to improve estimation for the individual participants. The advantages of hierarchical estimation relative to individual estimation can be seen by comparing Figure 2A and 2B. In situations with only a limited number of observations per participant, the individual model tends to overfit the data. As a result, parameter estimates are typically more variable than the true values that generated the data (grey crosses). In hierarchical estimation, the population distribution **shrinks** extreme individual estimates—especially those that are estimated imprecisely—to the group mean. This results in less variable and on average more accurate estimates.

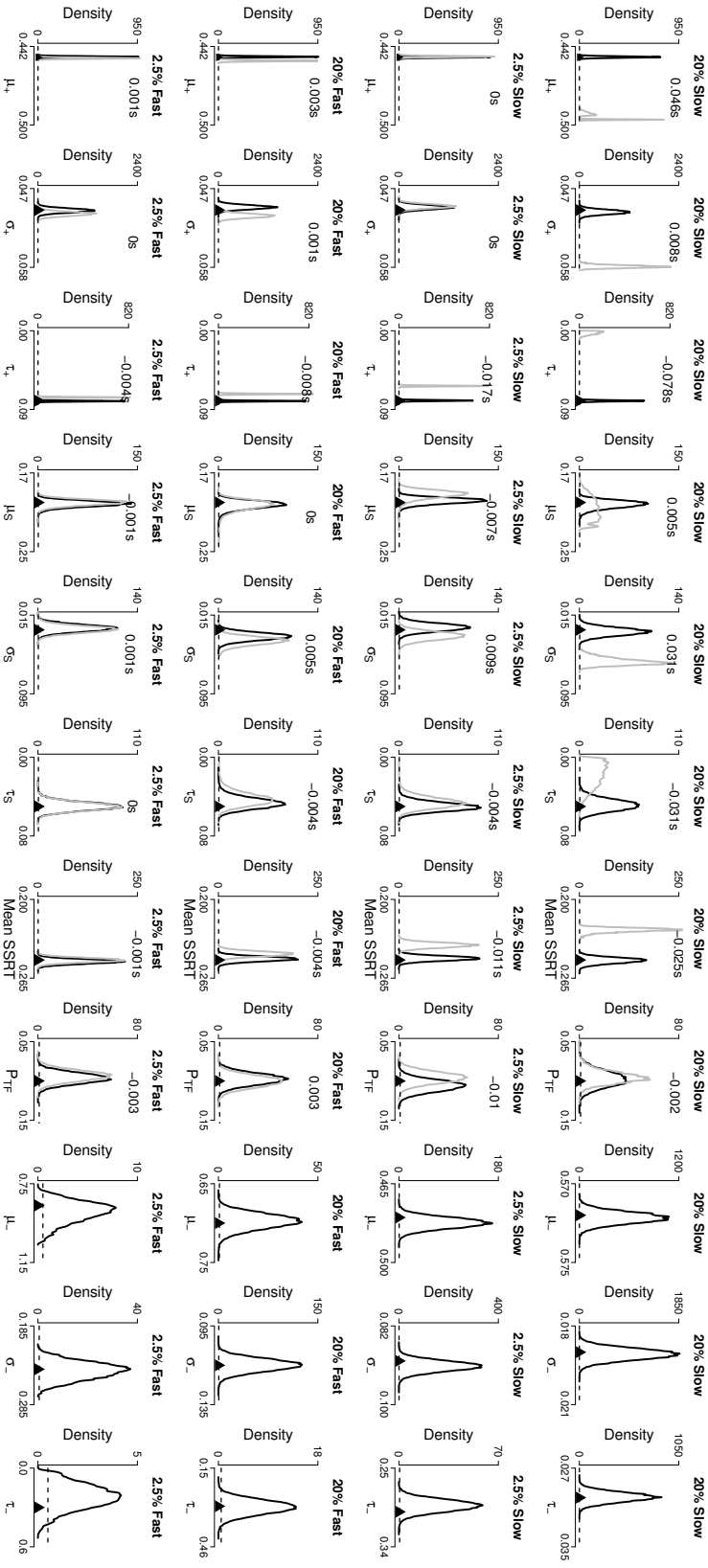


*Figure 2. Bias in parameter estimates as a result of go errors.* The black posterior distributions are computed with BEESTS3. The gray posterior distributions are computed with the misspecified BEESTS2 that does not account for go errors. The black triangles show the true values. The difference (in seconds) between the posterior means of the BEESTS2 and BEESTS3 estimates are shown in the upper right corners. Mean SSRT is computed as  $\mu_S + \tau_S$ . The subscripts + and - denote the matching and mismatching go runners, respectively.

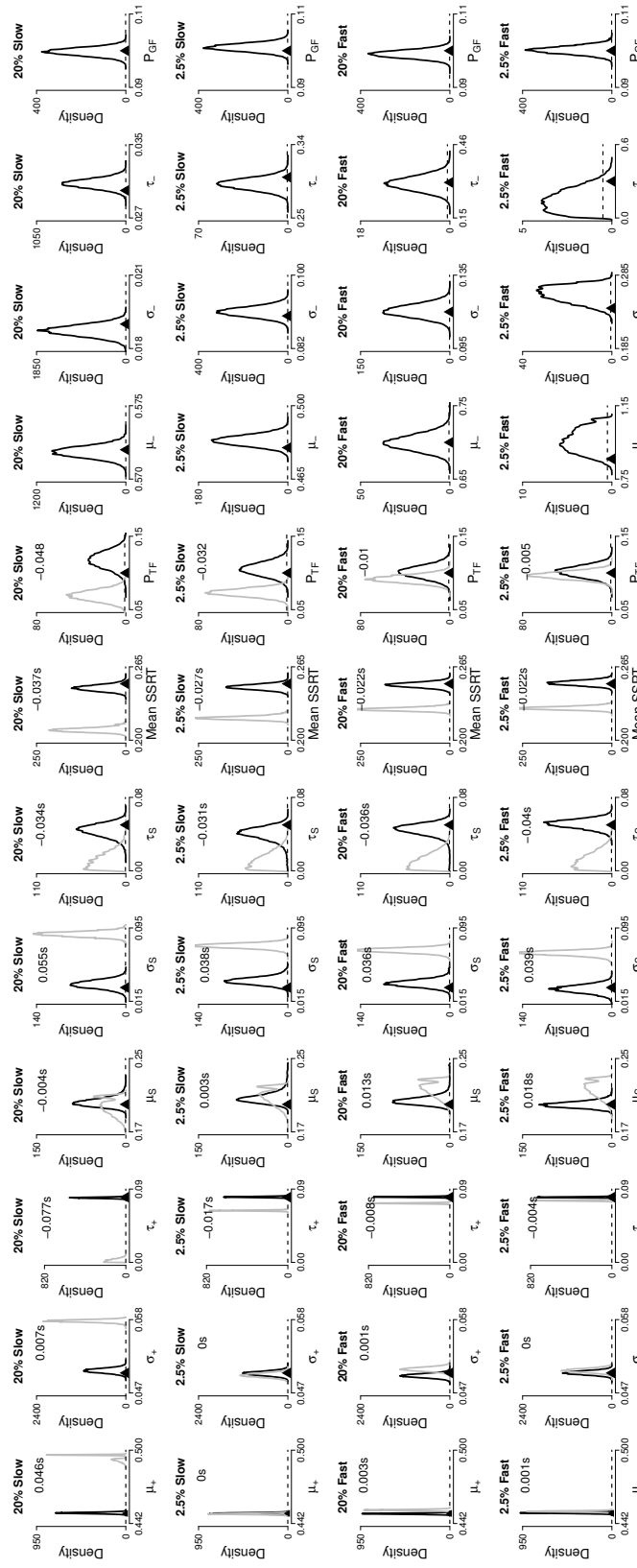


Figure 3. Bias in parameter estimates as a result of go failures and go errors. The black posterior distributions are computed with BEETS3-GF. The gray posterior distributions are computed with the misspecified BEETS2 that does not account for go failures and go errors. The black triangles show the true values. The difference (in seconds) between the posterior means of the BEETS2 and BEETS3-GF estimates are shown in the upper right corners. Mean SSRT is computed as  $\mu_S + \tau_S$ . The subscripts + and - denote the matching and mismatching go runners, respectively.

$$\mu_{+,E_j} \sim \text{Truncated-Normal}(\mu_{\mu_{+E}}, \sigma_{\mu_{+E}})[0, 4],$$

$$\mu_{-,E_j} \sim \text{Truncated-Normal}(\mu_{\mu_{-E}}, \sigma_{\mu_{-E}})[0, 4],$$

$$\mu_{+,D_j} \sim \text{Truncated-Normal}(\mu_{\mu_{+D}}, \sigma_{\mu_{+D}})[0, 4],$$

$$\mu_{-,D_j} \sim \text{Truncated-Normal}(\mu_{\mu_{-D}}, \sigma_{\mu_{-D}})[0, 4],$$

$$\sigma_{+,E_j} \sim \text{Truncated-Normal}(\mu_{\sigma_{+E}}, \sigma_{\sigma_{+E}})[0, 4],$$

$$\sigma_{-,E_j} \sim \text{Truncated-Normal}(\mu_{\sigma_{-E}}, \sigma_{\sigma_{-E}})[0, 4],$$

$$\sigma_{+,D_j} \sim \text{Truncated-Normal}(\mu_{\sigma_{+D}}, \sigma_{\sigma_{+D}})[0, 4],$$

$$\sigma_{-,D_j} \sim \text{Truncated-Normal}(\mu_{\sigma_{-D}}, \sigma_{\sigma_{-D}})[0, 4],$$

$$\tau_{+,E_j} \sim \text{Truncated-Normal}(\mu_{\tau_{+E}}, \sigma_{\tau_{+E}})[0, 4],$$

$$\tau_{-,E_j} \sim \text{Truncated-Normal}(\mu_{\tau_{-E}}, \sigma_{\tau_{-E}})[0, 4],$$

$$\tau_{+,D_j} \sim \text{Truncated-Normal}(\mu_{\tau_{+D}}, \sigma_{\tau_{+D}})[0, 4],$$

$$\tau_{-,D_j} \sim \text{Truncated-Normal}(\mu_{\tau_{-D}}, \sigma_{\tau_{-D}})[0, 4],$$

$$\mu_{S_j} \sim \text{Truncated-Normal}(\mu_{\mu_S}, \sigma_{\mu_S})[0, 4],$$

$$\sigma_{S_j} \sim \text{Truncated-Normal}(\mu_{\sigma_S}, \sigma_{\sigma_S})[0, 4],$$

$$\tau_{S_j} \sim \text{Truncated-Normal}(\mu_{\tau_S}, \sigma_{\tau_S})[0, 4],$$

$$P_{TF_j} \sim \text{Normal}(\mu_{P_{TF}}, \sigma_{P_{TF}}),$$

$$P_{GF_j} \sim \text{Normal}(\mu_{P_{GF}}, \sigma_{P_{GF}}).$$

We assigned truncated-normal prior distributions to the population means.

$$\mu_{\mu_{+E}}, \mu_{\mu_{-E}}, \mu_{\mu_{+D}}, \mu_{\mu_{-D}} \sim \text{Truncated-Normal}(0.5, 1)[0, 4],$$

$$\mu_{\sigma_{+E}}, \mu_{\sigma_{-E}}, \mu_{\sigma_{+D}}, \mu_{\sigma_{-D}} \sim \text{Truncated-Normal}(0.1, 1)[0, 4],$$

$$\mu_{\tau_{+E}}, \mu_{\tau_{-E}}, \mu_{\tau_{+D}}, \mu_{\tau_{-D}} \sim \text{Truncated-Normal}(0.1, 1)[0, 4],$$

$$\mu_{\mu_S} \sim \text{Truncated-Normal}(0.5, 1)[0, 4],$$

$$\mu_{\sigma_S} \sim \text{Truncated-Normal}(0.1, 1)[0, 4],$$

$$\mu_{\tau_S} \sim \text{Truncated-Normal}(0.1, 1)[0, 4],$$

$$\mu_{P_{TF}}, \mu_{P_{GF}} \sim \text{Normal}(-1.5, 1).$$

We assigned exponential prior distributions to the population standard deviations.

$$\sigma_{\mu_{+E}}, \sigma_{\mu_{-E}}, \sigma_{\mu_{+D}}, \sigma_{\mu_{-D}} \sim \text{Exponential}(1),$$

$$\sigma_{\sigma_{+E}}, \sigma_{\sigma_{-E}}, \sigma_{\sigma_{+D}}, \sigma_{\sigma_{-D}} \sim \text{Exponential}(1),$$

$$\sigma_{\tau_{+E}}, \sigma_{\tau_{-E}}, \sigma_{\tau_{+D}}, \sigma_{\tau_{-D}} \sim \text{Exponential}(1),$$

$$\sigma_{\mu_S} \sim \text{Exponential}(1),$$

$$\sigma_{\sigma_S} \sim \text{Exponential}(1),$$

$$\sigma_{\tau_S} \sim \text{Exponential}(1),$$

$$\sigma_{P_{TF}}, \sigma_{P_{GF}} \sim \text{Exponential}(1).$$

### Parameter Inference: Full Posterior Distributions

Figure 4 shows the posterior distribution of the population means obtained with BEESTS2, BEESTS3, and BEESTS3-GF. Figure 5 shows the posterior distribution of the population standard deviations obtained with BEESTS2, BEESTS3, and BEESTS3-GF.

Figure 6 and Figure 7 show the posterior distributions of two participants, one with 1.5% go omissions and 32% go errors, and the other with 0% go omissions and 30% go errors.

### Goodness-of-Fit

**Go RT and Signal-Respond RT Distributions.** Figure 8 shows the results of the posterior predictive simulations for BEESTS3-GF using the cumulative distribution function (CDF) of go RTs (upper panels) and signal-respond RTs (lower panels), separately for left (left panels) and right stimuli (right panels). The observed and predicted CDFs were averaged across participants. For brevity, go RTs were collapsed between the two difficulty conditions and signal-respond RTs were collapsed across SSDs.

Thick dashed and dotted lines show the CDF of the observed “LEFT” and “RIGHT” responses, respectively. Black circles show five percentiles ( $10^{th}$ ,  $30^{th}$ ,  $50^{th}$ ,  $70^{th}$  and  $90^{th}$ ) of the distributions. Thin dashed and dotted lines show the CDF of the predicted “LEFT” and “RIGHT” responses, respectively, averaged across the 100 replications. For each percentile, the gray bullets show the 100 predicted percentiles. Note that the upper asymptotes of the CDFs (i.e., their heights on the right) indicate the probability of the corresponding response. For go RTs they correspond to the probability of a correct and error response and add to one. For signal-respond RTs they also correspond to the probability of a correct and error response, which add to the response rate.

As indicated by the upper asymptote of the CDF of go RTs, BEESTS3-GF slightly under-predicted go-error rate for left stimuli and over-predicted go-error rate for right stimuli, likely as a result of a small response bias that we did not allow for in our modeling (i.e., by estimating different parameters for left and right runners). The model also provided very variable predictions for the  $90^{th}$  percentile of incorrect signal-respond RTs in response to right stimuli, probably as a result of scarce data. In all other respects, the predicted CDFs very closely approximated the observed CDFs, indicating that BEESTS3-GF provided an

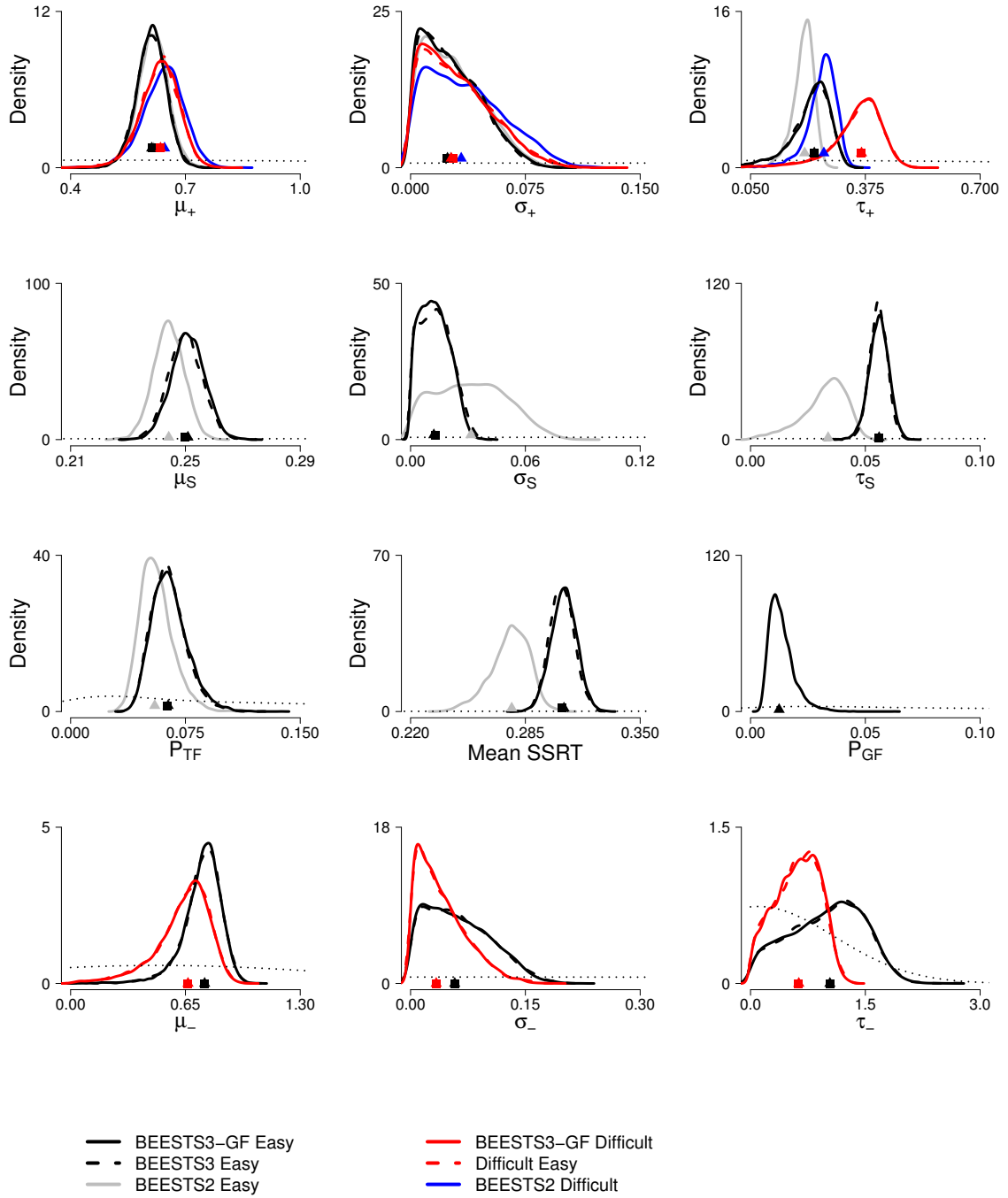


Figure 4. Posterior distributions of the population means obtained with BEESTS2, BEESTS3, and BEESTS3-GF. Posteriors distribution shown with solid gray and blue lines are computed with BEESTS2 in the Easy and Difficult conditions, respectively. Posteriors shown with dashed black and red lines are computed with BEESTS3 in the Easy and Difficult conditions, respectively. Posteriors shown with solid black and red lines are computed with BEESTS3-GF in the Easy and Difficult conditions, respectively. The dotted lines show the prior distributions. The triangles show the posterior medians. Mean SSRT is computed as  $\mu_S + \tau_S$ . The subscripts + and - denote the matching and mismatching go runners, respectively.

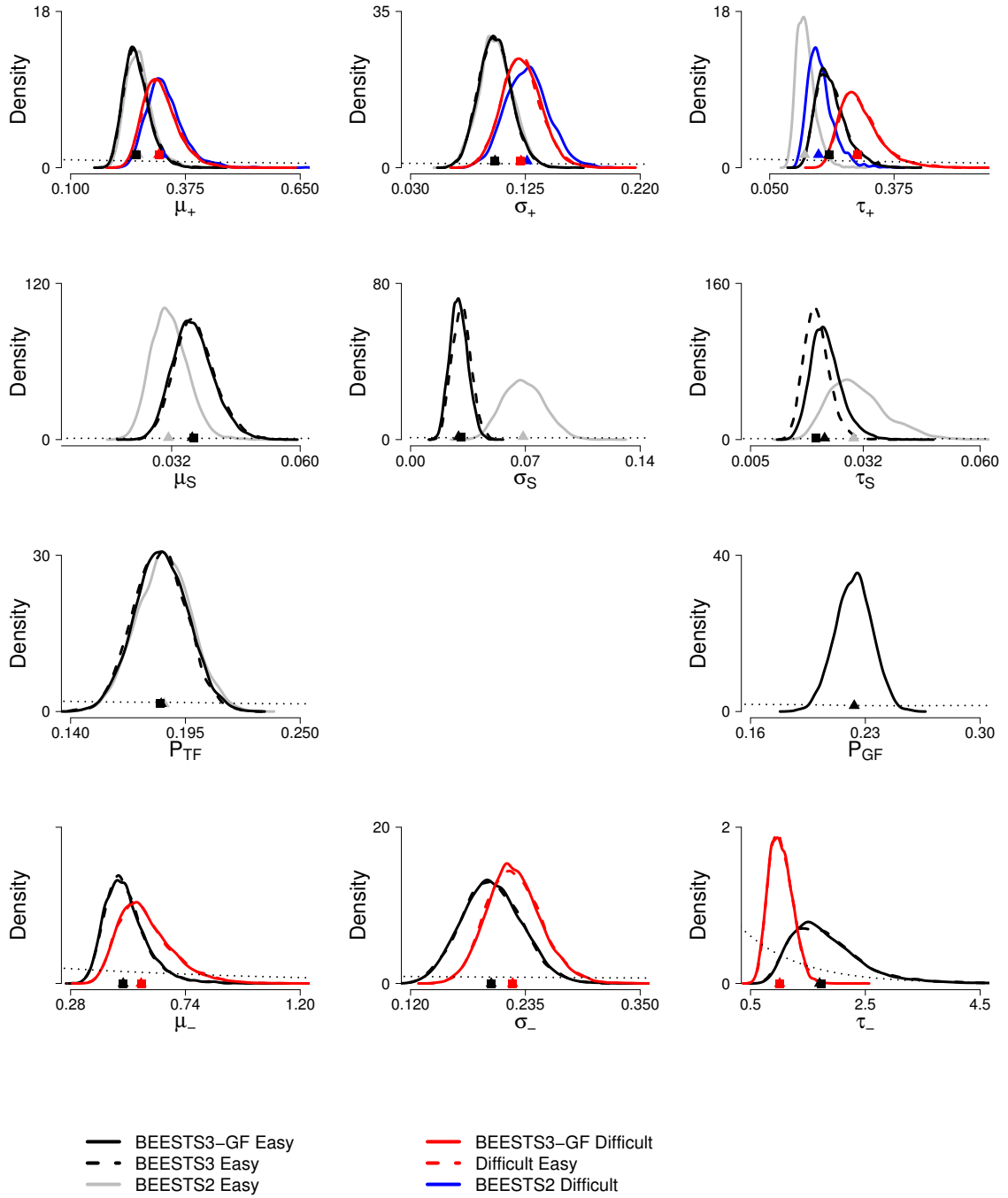


Figure 5. Posterior distributions of the population standard deviations obtained with BEESTS2, BEESTS3, and BEESTS3-GF. Posteriors distribution shown with solid gray and blue lines are computed with BEESTS2 in the Easy and Difficult conditions, respectively. Posteriors shown with dashed black and red lines are computed with BEESTS3 in the Easy and Difficult conditions, respectively. Posteriors shown with solid black and red lines are computed with BEESTS3-GF in the Easy and Difficult conditions, respectively. The dotted lines show the prior distributions. The triangles show the posterior medians. The subscripts + and – denote the matching and mismatching go runners, respectively.

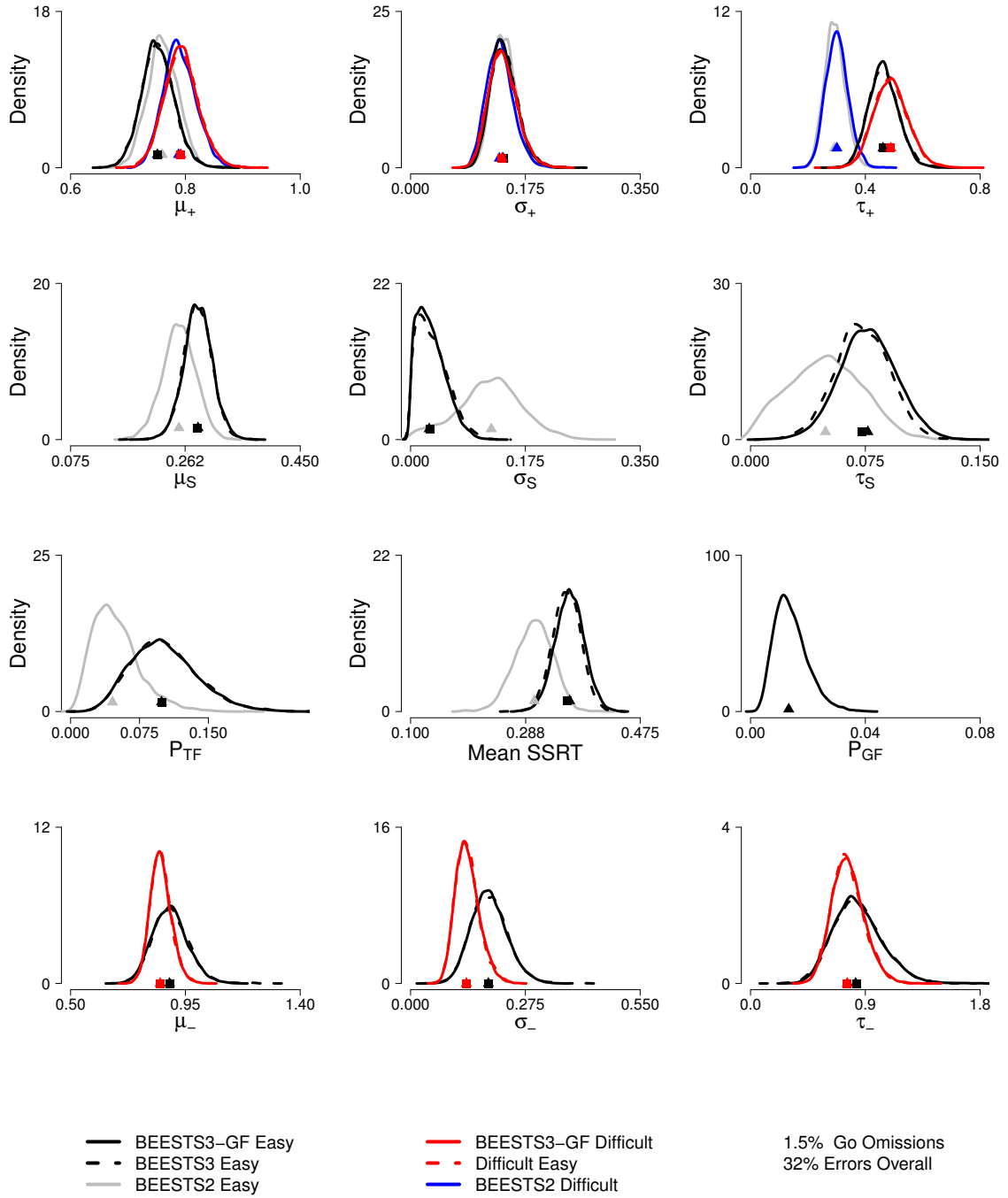


Figure 6. Posterior distributions for a single participant with 1.5% go omissions and 32% go errors. Posteriors distribution shown with solid gray and blue lines are computed with BEESTS2 in the Easy and Difficult conditions, respectively. Posteriors shown with dashed black and red lines are computed with BEESTS3 in the Easy and Difficult conditions, respectively. Posteriors shown with solid black and red lines are computed with BEESTS3-GF in the Easy and Difficult conditions, respectively. The triangles show the posterior medians. Mean SSRT is computed as  $\mu_S + \tau_S$ . The subscripts + and - denote the matching and mismatching go runners, respectively.

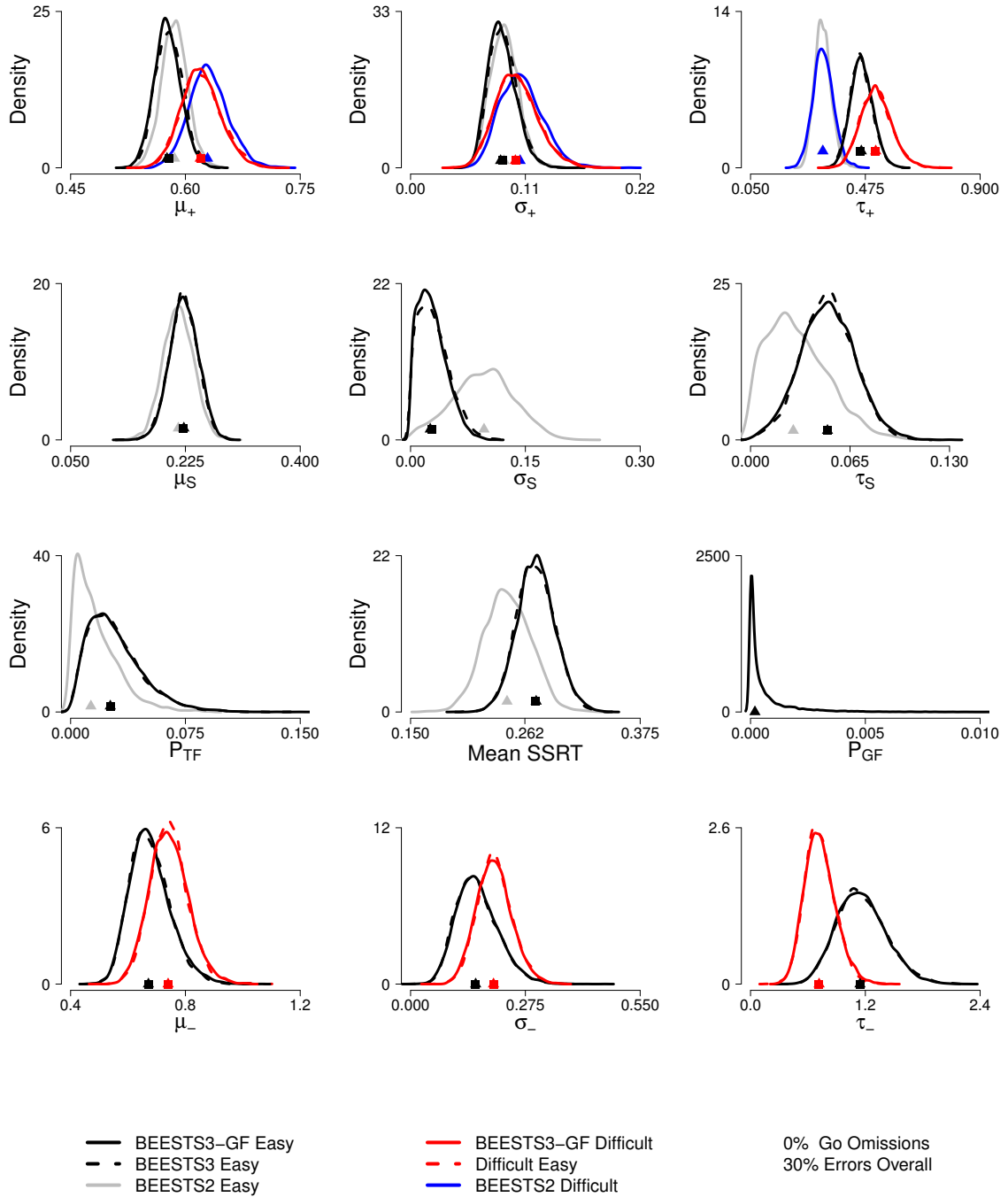


Figure 7. Posterior distribution for a single participant with 0% go omissions and 30% go errors. Posteriors distribution shown with solid gray and blue lines are computed with BEESTS2 in the Easy and Difficult conditions, respectively. Posteriors shown with dashed black and red lines are computed with BEESTS3 in the Easy and Difficult conditions, respectively. Posteriors shown with solid black and red lines are computed with BEESTS3-GF in the Easy and Difficult conditions, respectively. The triangles show the posterior medians. Mean SSRT is computed as  $\mu_S + \tau_S$ . The subscripts + and - denote the matching and mismatching go runners, respectively.

adequate description of the observed go RT and signal-respond RT distributions. The results of the posterior predictive simulations for BEESTS3 were essentially identical to the BEESTS3-GF results, and are not presented.

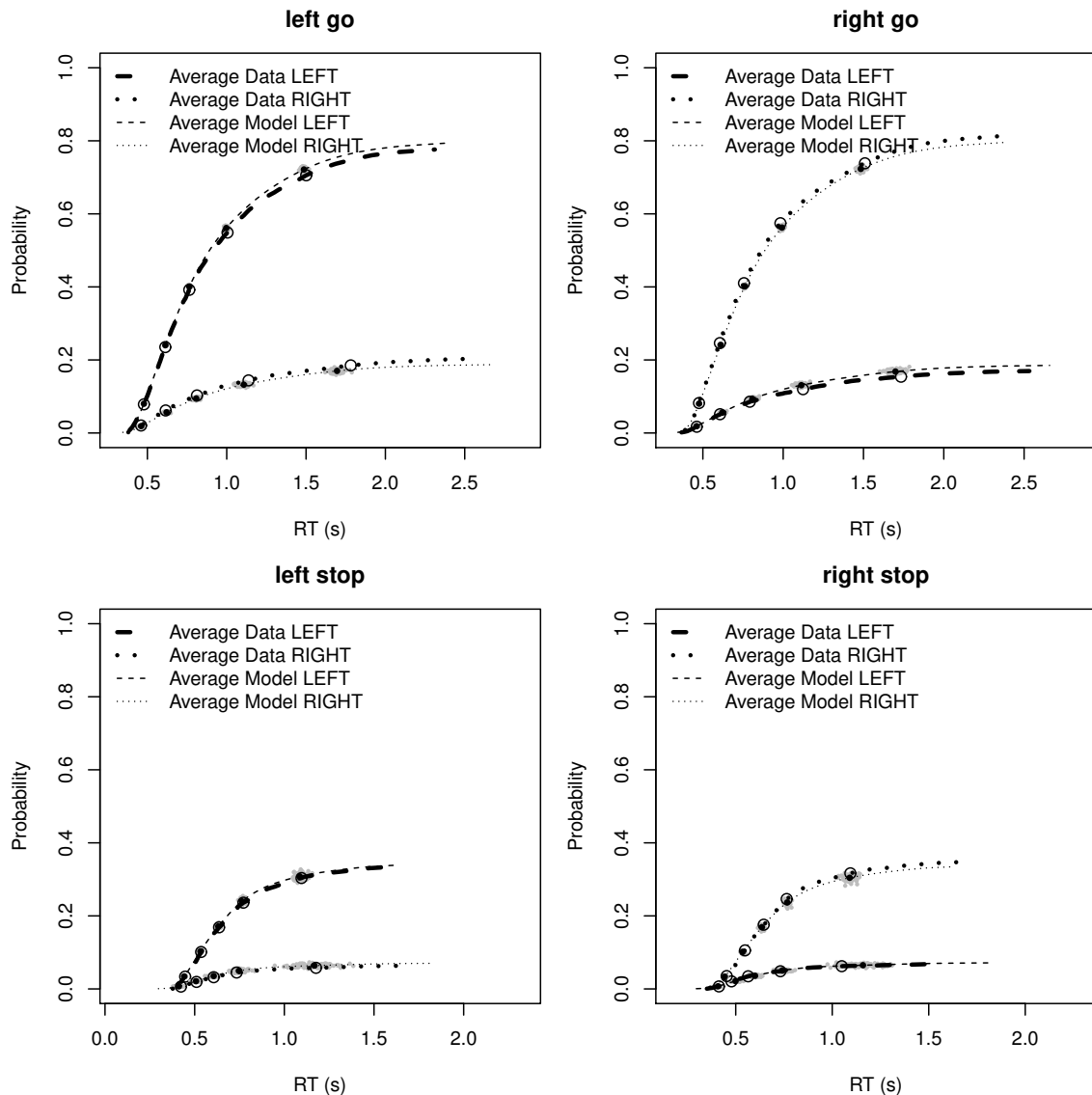


Figure 8. Observed vs. predicted cumulative distribution functions (CDF) of go RTs (top panels) and signal-respond RTs (bottom panels) for BEESTS3-GF.

Figure 9 shows the results of the posterior predictive simulations for BEESTS2 using the CDF of go RTs and signal-respond RTs. Note that Figure 9 does not distinguish between correct and incorrect responses as BEESTS2 does not account for go errors. As indicated by the upper asymptote of the CDF of signal-respond RTs, BEESTS2 slightly over-predicted signal-respond rate for left stimuli. In all other respects, the predicted CDFs very closely

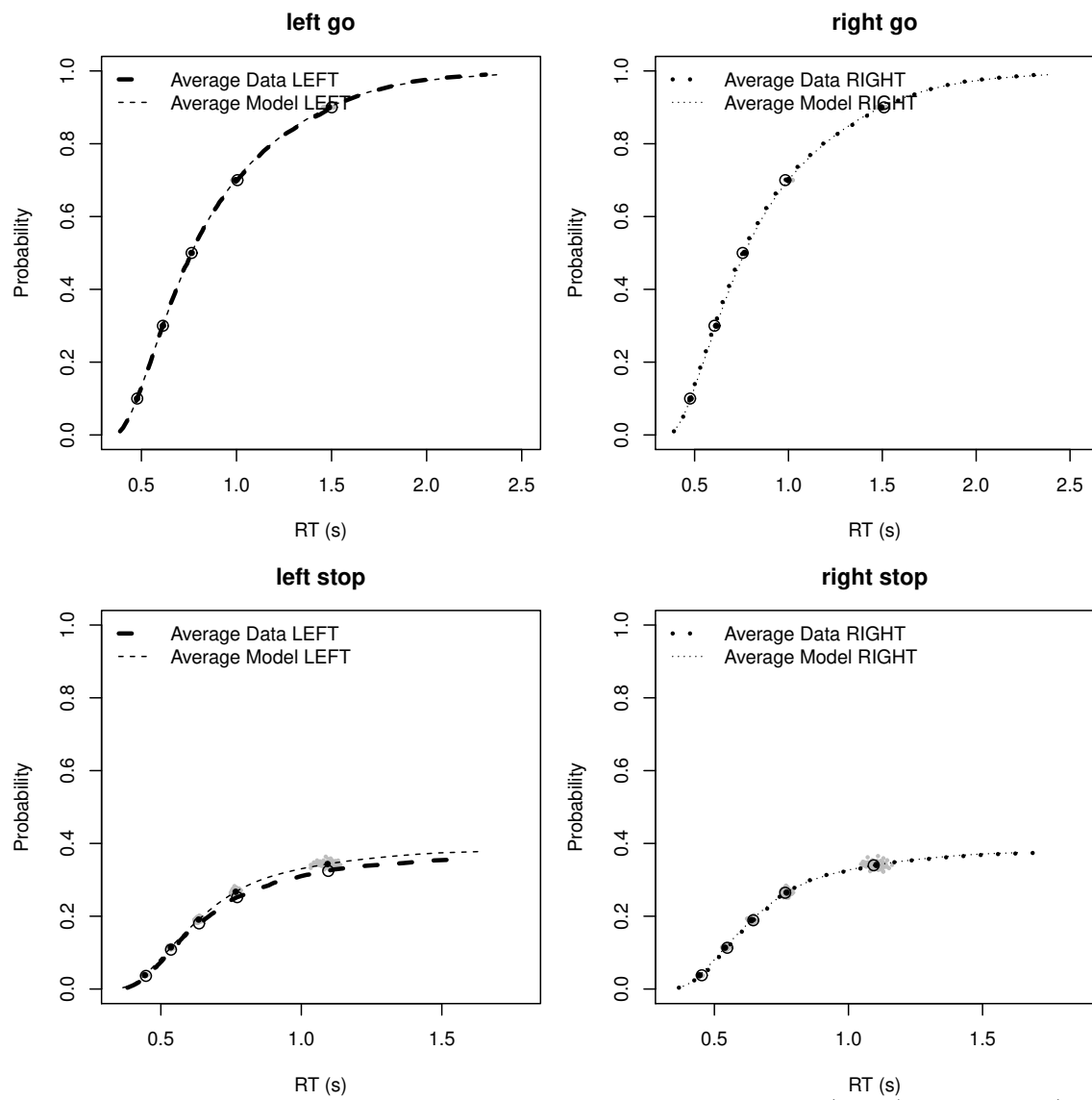


Figure 9. Observed vs. predicted cumulative distribution functions (CDF) of go RTs (top panels) and signal-respond RTs (bottom panels) for BEESTS2.

approximated the observed CDFs.